The Symmetry-Broken Formalism Applied to the Electronic Structure of an Iminosemiquinone Copper(II) Catalyst: A Key to the Qualitative Understanding of Its Reactivity

Vinzenz Bachler,* Phalguni Chaudhuri, and Karl Wieghardt[a]

Abstract: A concise outline of the known derivation of the singlet–triplet energy-gap equations within the symmetry-broken wavefunction framework is given. They allow a computation of the singlet–triplet energy gap for molecules that exhibit a weak antiferromagnetic coupling of electrons. The accuracy of the equations is assessed by computation of the singlet–triplet gaps in model Na_2 molecules. Various antiferromagnetic coupling strengths are simulated by the use of different Na–Na bond lengths in the computations. The singlet–triplet energy gaps obtained with the different equations are compared with the gaps computed with the more accurate coupled-cluster methods. Subsequently, the equations are applied to an iminosemiquinone copper(II) complex found previously to have remarkable catalytic properties. The application is performed by employing wavefunction equations but with quantities computed within the density functional framework. The electronic ground state of this complex is computed to be a singlet state, which is also the experimental finding. Moreover, the experimental geometry and the singlet–triplet gap are reasonably reproduced by the computation. A straightforward method to determine the magnetic orbitals is suggested and applied. We illustrate that the form of the magnetic orbitals indicates in a qualitative manner that hydrogen-atom abstraction should be a major reaction pathway of the iminosemiquinone copper(II) complex. Hydrogen-atom abstraction has been suggested previously to be the rate-determining step in a catalytic process initiated by the iminosemiquinone copper(II) complex. The results support the notion that the form of the magnetic orbitals might be a qualitative indicator for the reactivity of molecules that exhibit weak antiferromagnetic coupling.

Keywords: antiferromagnetic coupling · copper · density functional calculations · magnetic properties · radicals · symmetry-broken formalism

Introduction

Recently, the iminosemiquinone copper(II) complex $[Cu^{II}(L^2)(NEt)_3]$ (**1**) was synthesized.[1] A remarkable feature of **1** is its ability to selectively transform primary alcohols, except CH_3OH, in the presence of O_2 to aldehydes and H_2O_2.[1] The authors propose the mechanism given in Scheme 1 for this catalytic process, in which $(L^3)^{3-}$ represents the one-electron reduced, diamagnetic form of the radical $(L^2)^{2-}$. In this mechanism the rate-determining step is a hydrogen-atom abstraction from the α-carbon atom of the alcohol, bonded as an alcoholate to the copper atom. The remarkable reactivity of complex **1** is supplemented by interesting magnetic properties. The temperature-dependent magnetic moments of **1** were fitted to the Heisenberg Hamiltonian $H = -2JS_{Cu} \cdot S_{Lig}$ ($S_{Cu} = S_{Lig} = ½$) and an exchange coupling constant of $J = -137\ cm^{-1}$ was determined, indicative of a singlet ground state of **1**. Thus, a rather small singlet–triplet gap exists in complex **1**. At low temperatures, the electronic singlet state prevails.[1] At ambient temperatures, however, the triplet state is populated.[1] The observed small singlet–triplet gap indicates that a weak antiferromagnetic coupling operates in complex **1**.

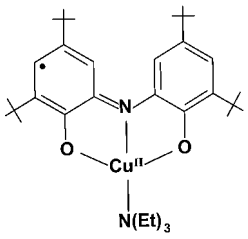

1

The computation of the electronic properties of such complexes is, in general, a difficult problem. Electronic wavefunctions are needed which allow electrons of opposite spins to become localized in different spatial regions of the molecule.[2] Thus, a careful treatment of the electron correlation is mandatory in the description of the electronic properties of these molecules. Staemmler and co-workers employed the coupled electron pair approximation in a high-quality ab initio approach to compute the coupling constants J.[3] Several oxo-bridged Cr^{III}, V^{III}, and Ti^{III} complexes that

[a] Dr. V. Bachler, Prof. Dr. P. Chaudhuri, Prof. Dr. K. Wieghardt
Max-Planck-Institut für Strahlenchemie
Postfach 101365, D-45413 Mülheim an der Ruhr (Germany)
Fax: (+49) 208-3063951
E-mail: bachler@mpi-muelheim.mpg.de

0947-6539/01/0702-0404 $ 17.50+.50/0

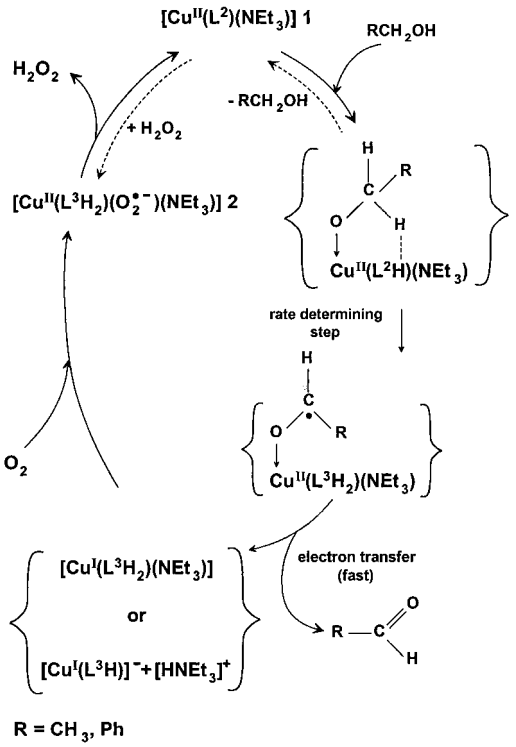

Scheme 1. The proposed catalytic cycle[1] for the oxidation of alcohols with catalyst **1**. Notice the rate-determining hydrogen-atom abstraction step.

exhibit a weak antiferromagnetic coupling were treated.[3] The computed J values are in good agreement with the values obtained from magnetic measurements.[3].Staemmler and co-workers also treated the magnetic exchange coupling in chlorine-bridged binuclear Co^{II} complexes.[4] A characteristic feature of their work is that spin-orbit coupling and Zeeman splitting is explicitly considered in the computations.[4] Moreover, the temperature dependence of the magnetic susceptibilities is computed.[4] A much less rigorous but simpler theoretical procedure to treat molecules with a weak antiferromagnetic coupling is the symmetry-broken formalism introduced by Noodleman and co-workers.[5] This approach has been successfully applied not only in the wavefunction,[6] but also in the framework of density functional theory (DFT).[7]

In this paper, we first outline the known derivation of the approximate equations for a singlet–triplet gap in the formalism of broken symmetry. Then, we apply the equations to the molecule Na_2 in which the bond has been elongated by various amounts. By the use of this simple scheme, we simulate antiferromagnetic couplings of different strengths. We assess the accuracy of the approximate singlet–triplet gap equations by comparison with results obtained from accurate ab initio methods. The major objective of this paper, however, is to understand qualitatively the electronic properties of complex **1**. We pursue this aim by application of the symmetry-broken wavefunction formalism; however, we employ quantities derived from density functional calculations.

Abstract in German: *Die bekannte Ableitung von Formeln für die Singulett–Triplett Energieaufspaltung im symmetriegebrochenen Wellenfunktionsformalismus wird zusammengefaßt. Die Formeln erlauben die Singulett–Triplet Energieaufspaltung für Moleküle zu berechnen deren Elektronen schwach antiferromagnetisch gekoppelt sind. Die Genauigkeit der Formeln für unterschiedliche Kopplungstärken wird überprüft. Dies geschieht durch die Berechnung der Singulett–Triplett Energieaufspaltung in Na_2 Molekülen mit unterschiedlichen Na–Na Bindungslängen und einem Vergleich mit genaueren Singulett–Triplett Energieaufspaltungen, die mit Coupled-Cluster Methoden berechnet wurden. Anschließend werden die Formeln auf einen Iminosemichinon Kupfer(II) Komplex angewendet, der bemerkenswerte katalytische Eigenschaften besitzt. In Übereinstimmung mit dem Experiment, wird der electronische Grundzustand als ein Singulett Zustand berechnet. Die experimentelle Geometrie und die Singulett–Triplett Energieaufspaltung werden durch die Rechnung vernünftig wiedergegeben. Ein einfaches Verfahren zur Bestimmung der magnetischen Orbitale wird vorgeschlagen und angewendet. Die Form der magnetischen Orbitale zeigt qualitative an, daß Wasserstoffatomabstraktion ein Hauptreaktionsweg des Iminosemichinon Kupfer(II) Komplexes sein sollte. Die Ergebnisse unterstützen die Vorstellung, daß die Form der magnetischen Orbitale ein qualitativer Indikator für die Reaktivität von Molekülen mit schwacher antiferromagnetischer Kopplung sein könnte.*

Results and Discussion

A simple derivation of the symmetry-broken formalism for molecules that exhibit a weak antiferromagnetic coupling

Restricted and unrestricted MO Slater determinants: Consider a molecule in its singlet ground state: in most standard quantum chemical procedures, a closed-shell, restricted Hartree–Fock (RHF) Slater determinant serves as a first-order approximation to compute this electronic state. This wavefunction is subsequently improved by consideration of electron correlation in the computation. The restricted closed-shell RHF Slater determinant is restricted because the α and β electrons of an electron pair occupy not different but the same molecular orbitals (MOs) in the Slater determinant. Consequently, the spin-coupled electrons of an electron pair are forced to occupy the same spatial regions in a molecule. Thus, the RHF Slater determinant is a good first-order approximation for molecules that exhibit a strong antiferromagnetic coupling. Such a coupling operates in the majority of organic molecules. Many transition metal complexes, however, exhibit a weak antiferromagnetic coupling. This often implies that two weakly coupled electrons with α and β spin occupy *different* spatial regions in a molecule. Noodleman suggested that for this type of transition metal complex the electronic wavefunction is well approximated by the unrestricted Hartree–Fock (UHF) Slater determinant.[5] The characteristic feature of a UHF Slater determinant is that the space parts of α and β-spin orbitals can be different.[8] If a weak antiferromagnetic coupling operates, the UHF Slater determinant leads to an energy which is *lower* than the energy for

the corresponding RHF Slater determinant. Noodleman designates such a UHF Slater determinant as the *symmetry-broken* wavefunction for a transition metal complex.[9].The symmetry is broken because the MOs in the UHF Slater determinant do not necessarily transform as the irreducible representations of the point group of the transition metal complex. Moreover, the spin symmetry is broken because the UHF Slater determinant does not describe a pure spin state[10] but a state of mixed spin. Nevertheless, Noodleman showed that from such a symmetry-broken wavefunction one can obtain equations to compute the singlet–triplet energy splittings in transition metal complexes that exhibit a weak antiferromagnetic coupling.[11].

Three equations for the singlet–triplet energy splitting: Consider the symmetry-broken wavefunction Ψ_b^{UHF}, computed by means of the unrestricted Hartree–Fock (UHF) method.[8] Such a Ψ_b^{UHF} is not an eigenfunction of the total spin operator S^2, a finding which is valid for any UHF Slater determinant.[10] Nevertheless, one can expand Ψ_b^{UHF} into a set of Φ_i which are eigenfunctions of the molecular Hamiltonian H[12] and of S^2 [Eq. (1)].[13]

$$\Psi_b^{UHF} = \sum_{i=1}^{N} c_i \Phi_i \tag{1}$$

Amos and Hall have shown that a UHF Slater determinant, with a spin quantum number of about $S_i = n$, contains only Φ_i whose spin multiplicities $2S_i+1$ are determined by $S_i = n$, $S_i = n+1$, $S_i = n+2$, and so forth.[14] Thus, for a Ψ_b^{UHF} whose major component has a spin quantum number of $S_b = 0$, the sum in Equation (1) ranges only over those Φ_{iS} for which $S_i = 0$, $S_i = 1$, $S_i = 2, \ldots$ holds. For a definite number of electrons, this set of S_i gives rise to the spin multiplicities recorded in the vertical line of the spin-branching diagram.[15] The symmetry-broken Ψ_b^{UHF} is an eigenfunction of the S_z spin operator with eigenvalue $M_s = 0$. Consequently, only Φ_i appear in the sum of Equation (1) for which $M_s = 0$ holds. The variational energy E_b^{UHF} is the expectation value of Ψ_b^{UHF} over the molecular Hamiltonian H. By means of Equation (1) and utilization of the properties that the Φ_i are orthonormal and eigenfunctions of H with eigenvalue E_i, we obtain Equation (2) for E_b^{UHF}.[16]

$$E_b^{UHF} = \langle \Psi_b^{UHF} | H | \Psi_b^{UHF} \rangle = c_s^2 E_s + c_t^2 E_t + \sum_i{}' c_i^2 E_i \tag{2}$$

Here, E_s and E_t are the exact energies of the singlet ground state and of the first excited triplet state, respectively. The corresponding expansion coefficients are designated by c_s and c_t. The prime at the summation in Equation (2) symbolizes that contributions for the singlet ground state and for the first excited triplet state are omitted. Thus, the energy E_b^{UHF} for the symmetry-broken electronic state is a linear combination of the exact energies of the various electronic states with spin multiplicities other than singlet.[16] Equation (2) leads immediately to a simple expression for the exact singlet ground state energy E_s [Eq. (3)]:

$$E_s = \frac{E_b^{UHF} - \sum_i{}' c_i^2 E_i - c_t^2 E_t}{c_s^2} \tag{3}$$

This formula is of interest for a computation of the singlet ground state energy, provided a symmetry-broken UHF wavefunction can be found. This concept has been pursued by Ovchinnikov and Labanowski[17] who neglected the sum in Equation (3) and used a variationally determined E_t to compute an approximate E_s. They calculated its dependence from the bending and stretching vibrational modes for the molecules CH_2 and O_2, respectively.[17] Wittbrod and Schlegel also applied the simplified Equation (3) to compute the potential energy curves for the hydrogen fluoride and the C–H dissociation of methane.[18] They conclude that the qualitative behavior of these curves is incorrect relative to more exact potential energy curves.[18] Subtraction of E_t from both sides of Equation (3) gives an exact equation for the singlet–triplet splitting [Eq. (4)]:

$$E_s - E_t = \frac{E_b^{UHF} - \sum_i{}' c_i^2 E_i - (c_s^2 + c_t^2) E_t}{c_s^2} \tag{4}$$

From the normalization of Ψ_b^{UHF} and Equation (1) we derive Equation (5). By substitution of Equation (5) into Equation (4), we obtain an equation for the exact singlet–triplet gap, namely Equation (6).

$$c_s^2 + c_t^2 = 1 - \sum_i{}' c_i^2 \tag{5}$$

$$E_s - E_t = \frac{E_b^{UHF} - E_t + \sum_i{}' c_i^2 (E_t - E_i)}{c_s^2} \tag{6}$$

An approximate $E_s - E_t$ can be derived from Equation (6) by making the following assumptions: i) The spin contamination of Ψ_b^{UHF} by electronic states higher than the first excited triplet state is negligible. ii) The energy differences $E_t - E_i$ on the right hand side of Equation (6) are small. iii) The exact triplet energy E_t in the numerator of Equation (6) is approximated by the variational energy $\tilde{E}_t$ obtained by means of the restricted open-shell Hartree–Fock (ROSHF) method. Assumption (i) implies small expansion coefficients c_i for electronic states higher than the first exited triplet state. The smallness of these c_i was verified for several molecules.[19] Condition (ii) should be operative in transition metal complexes which frequently exhibit a dense spacing of electronic states. This is in contrast to the majority of organic molecules. Conditions (i) and (ii) imply that for a treatment of transition metal complexes the sum in Equation (6) can be neglected. By the use of assumptions (i)–(iii) we obtain from Equation (6) an approximate equation for the singlet–triplet energy splitting, namely Equation (7):

$$E_s - E_t = \frac{E_b^{UHF} - \tilde{E}_t}{c_s^2} \tag{7}$$

In many transition metal complexes assumption (ii) holds and we can suppose that Equation (7) is adequate for the treatment of those compounds. In order to apply Equation (7), we have to determine c_s^2. For this purpose we

0947-6539/01/0702-0406 $ 17.50+.50/0 *Chem. Eur. J.* **2001**, *7*, No. 2

consider the expectation value over the spin operator S^2 computed with Ψ_b^{UHF}. By the use of Equation (1) and neglecting contributions from electronic states higher than the first excited triplet state, we can write Equation (8):

$$\langle \Psi_b^{UHF} | S^2 | \Psi_b^{UHF} \rangle = c_s^2 S_s(S_s+1) + c_t^2 S_t(S_t+1) \quad (8)$$

By neglecting those electronic states also in the normalization condition for Ψ_b^{UHF}, we obtain Equation (9):

$$c_s^2 + c_t^2 = 1 \quad (9)$$

In Equation (8) it is assumed that the symmetry-broken electronic state is a mixture of the singlet ground state and the first excited triplet state. Therefore, $S_s = 0$ and $S_t = 1$ hold. By combining Equations (8) and (9), we obtain Equation (10) for c_s^2 and substitution of Equation (10) into Equation (7) leads to Equation (11).

$$c_s^2 = 1 - \frac{\langle \Psi_b^{UHF} | S^2 | \Psi_b^{UHF} \rangle}{2} \quad (10)$$

$$E_s - E_t = \frac{2(E_b^{UHF} - \tilde{E}_t)}{2 - \langle \Psi_b^{UHF} | S^2 | \Psi_b^{UHF} \rangle} \quad (11)$$

This formula for the singlet triplet energy splitting has been obtained and applied by Ovchinikov and Labanowski.[20] Adamo et al. derived the same equation, which they applied to the magnetic exchange interaction in copper(II) μ_2-azido-bridged complexes.[21] One can assume that the spin polarization of the inner electrons can be neglected and only one α and one β orbital are nonorthogonal. This idea has already been pursued by Malrieu and co-workers.[22]. They obtained a simplified Equation (11) in which the square of the overlap of the magnetic orbitals appears instead of $\langle \Psi_b^{UHF} | S^2 | \Psi_b^{UHF} \rangle$. Malrieu and co-workers investigated model cases, such as H-He-H, as well as dinuclear copper complexes.[22] We can specify Equation (11) for the case of a weak antiferromagnetic coupling. For such a coupling, Ψ_b^{UHF} should comprise nearly equal parts of singlet and triplet wavefunctions. Therefore $\langle \Psi_b^{UHF} | S^2 | \Psi_b^{UHF} \rangle \approx 1$ holds and Equation (11) yields Equation (12) for the singlet–triplet gap:

$$E_s - E_t = 2(E_b^{UHF} - \tilde{E}_t) \quad (12)$$

This equation has been derived by Noodleman[11] and has been extensively applied in the past.[6, 7].In most applications $\tilde{E}_t$ is the high-spin energy computed with the UHF wavefunction, which is not an eigenfunction of the spin operator S^2. Hart et al. have pointed out that the ferromagnetic, the superexchange, and the ligand spin-polarization parts are contained in the exchange coupling constant provided the high-spin energy is derived from a spin-pure wavefunction.[6c] Moreover, for several model compounds, the most accurate exchange coupling constants were obtained by means of ROSHF energies for the high-spin state.[6c] Therefore, we employed the ROSHF triplet energy for $\tilde{E}_t$ to ensure that the three important contributions are contained in Equations (11) and (12). In the limit of a strong antiferromagnetic coupling, $\langle \Psi_b^{UHF} | S^2 | \Psi_b^{UHF} \rangle \approx 0$ holds and one obtains Equation (13) from Equation (11):

$$E_s - E_t = E_b^{UHF} - \tilde{E}_t \quad (13)$$

Thus, Equation (11) is a general formula for the singlet–triplet energy gap which holds for the whole range of antiferromagnetic coupling strengths.[20, 21] In the following section we assess the accuracy of Equations (11)–(13) by treating Na_2 molecules with elongated bonds. These model systems serve as a tool to simulate antiferromagnetic couplings of different strengths.

Applied computational methods for the model Na_2 molecules: All computations for Na_2 were performed by means of the Gaussian 98 suite of ab initio programs[23] and we used the standard 6-311G* Gaussian basis sets.[24] Thus, the valence orbitals of the Na atoms are of approximate triple-zeta quality and d polarization functions are provided.[24] We performed RHF calculations for the singlet ground state of Na_2 molecules in which various bond lengths are assumed and we obtained the total energies E_s^{RHF}. Subsequently, the stability of the RHF Slater determinant with respect to a symmetry-broken UHF solution was investigated. This was carried out by means of the formalism proposed by Seeger and Pople[25] which is referenced in Gaussian 98 by the keyword STABLE. We modified STABLE by the option OPT. This initiates the program to find the energy E_b^{UHF} for the UHF Slater determinant Ψ_b^{UHF} that describes the symmetry-broken electronic state.[23] The quantity $\tilde{E}_t$ in Equations (11)–(13) was derived by performing ROHF calculations for the first excited triplet state. For an assessment of the accuracy of Equations (11)–(13), accurate singlet–triplet energy differences are needed. They were obtained by means of the coupled-cluster method.[26] Single and double excitations and an estimate for triple excitations (CCSD(T)) were included.[26] We computed the energy $E_s^{CCSD(T)}$ of the singlet ground state and the energy $E_s^{CCSD(T)}$ of the first excited triplet state. The expectation values $\langle \Psi_b^{UHF} | S^2 | \Psi_b^{UHF} \rangle$ for the spin operator S^2 are routinely computed and printed out by the Gaussian 98 program.[23] The approximate singlet–triplet gap Equations (11)–(13) were obtained within the wavefunction framework. However, we applied them to the iminosemiquinone copper(II) complex **1** in the density functional theory (DFT) formalism, as described below. For this purpose we also employed Equations (11)–(13); however, we used quantities E_b^{UHF} and $\tilde{E}_t$ computed by means of the B3LYP DFT procedure.[27] Therefore, it is of interest to assess the accuracy of Equations (11)–(13) by applying them within the B3LYP DFT framework. We performed B3LYP calculations for the singlet ground state of Na_2 molecules with various bond lengths. This produced the corresponding energies E_s^{B3LYP}. Subsequently, the stability of the singlet solution with respect to a symmetry-broken solution was investigated. This was carried out by means of the formalism developed by Bauernschmitt and Ahlrichs,[28] as implemented in Gaussian 98.[23] If the singlet B3LYP solution is unstable, the program

finds the symmetry-broken B3LYP solution, which yields the energy E_b^{UB3LYP}. Thus, our adopted computational scheme is very similar to the procedure applied by Gäfenstein et al. who investigated the Bergman reaction by means of DFT computations.[29] The restricted DFT solution for the transition state was found to be unstable.[29] An unrestricted symmetry-broken DFT solution exists which is of lower energy than the restricted one.[29] This finding is a consequence of the singlet diradical character of the transition state.[29] The stability of the restricted DFT solution as a function of the various exchange correlation functionals has been carefully discussed.[29] For the approximate energy $\tilde{E}_t$ of the first excited triplet state, we employed $E_t^{ROB3LYP}$ computed by means of the restricted open-shell formalism.

The accuracy of the approximate singlet – triplet energy gap equations

The symmetry-broken wavefunction formalism: We have applied Equations (11) – (13) to Na_2 molecules with Na–Na bond lengths that are significantly longer than the experimental bond length of 3.078 Å.[30] By elongation of the Na – Na bond we simulate different antiferromagnetic coupling strengths between the 3s electrons of the Na atoms which form the σ bond. The computational results are recorded in Table 1. The data given in Entries 1 and 2 of Table 1 show that for all bond lengths, E_b^{UHF} is lower than E_s^{RHF}. This finding illustrates the well-known deficiency of the RHF Slater determinant. It does not describe the correct homolytic bond breaking of the Na–Na bond, but a heterolytic bond breaking that leads to the high-energy products Na^- and Na^+. The energy differences $E_b^{UHF} - E_s^{RHF}$ are slightly larger for the longer bond lengths considered. The finding that all E_b^{UHF} are lower than E_s^{RHF} indicates that a weak antiferromagnetic coupling operates in the distorted Na_2 molecules. In Entries 4 and 5 we have given the coupled-cluster energies $E_t^{CCSD(T)}$ and $E_s^{CCSD(T)}$ for the triplet and singlet state, respectively. Interestingly, the $E_t^{CCSD(T)}$ values are close to the quantities E_t^{ROHF} given in Entry 3. This agreement shows that E_t^{ROHF}, designated by $\tilde{E}_t$ in Equations (11) – (13), is a rather good approximation to the exact triplet energy E_t. In Entry 6 we give the energy differences $E_s^{CCSD(T)} - E_t^{CCSD(T)}$ which serve as reference singlet – triplet energy gaps. The singlet – triplet gaps obtained with the spin-corrected Equation (11) are given in Entry 8. We realize that over the whole range of coupling strengths, simulated Equation (11) performs with a uniform accuracy of about 62 %. A less uniform performance should hold for Equations (12) and (13), which describe the weak and strong antiferromagnetic coupling regimes, respectively. However, Entry 9 illustrates that Equation (12) also behaves uniformly over the whole range of coupling strengths, and an average accuracy of about 73 % is achieved. As expected, Equation (13) (Entry 10) behaves slightly better in the strong antiferromagnetic coupling case. For the largest distance of 6.0 Å, the smallest singlet – triplet energy difference of 302.4 cm^{-1} is computed. For this energy gap the spin-corrected Equation (11) and correspondingly the Noodleman equation [Eq. (12)] are quite accurate (73 %). At this largest distance, $\langle \Psi_b^{UHF} | S^2 | \Psi_b^{UHF} \rangle$ is close to unity (Entry 11). This indicates that Ψ_b^{UHF} can be considered as an equal mixture of singlet and triplet spin states. This finding might justify neglecting the higher spin multiplicities in Equations (6) and (8). The rather good performance of Equation (12) for a weak antiferromagnetic coupling is in agreement with the results already found by Hart et al.[6c] These authors performed configuration-interaction calculations to obtain the exchange coupling constants J for the model compounds H-He-H, $[H\text{-}F\text{-}H]^-$, and the molecule Cl_4Ti_2O. To simulate various antiferromagnetic coupling strengths, they also varied definite bond lengths in the molecules. Their constants J are the energy-gap values of Equation (12) but divided by two. The singlet – triplet gaps, obtained from accurate computations, are best reproduced by Equation (12), provided the ROHF energies for the high-spin state are employed.[6c] Our results are also substantiated by recent work of Ruiz et al. who computed singlet – triplet gaps for various dinuclear transition-metal complexes.[31] If a symmetry-broken UHF wavefunction is applied, Equation (11) produces gaps which are in agreement with the observed exchange coupling constants (see Table II in ref. [31]).

The wavefunction formalism applied with density functional quantities: Our B3LYP[27] results for the Na_2 molecules with elongated bonds are given in Table 2. For all distances, the

Table 1. The singlet – triplet gaps computed by means of Equations (11) – (13) for Na_2 molecules with various bond lengths. The different bond lengths simulate antiferromagnetic couplings of various strengths. Gaps obtained from coupled-cluster computations serve as a reference. At all coupling strengths, the spin-corrected Equations (11) and (12) perform with an almost uniform accuracy. As expected, Equation (13) performs slightly better in the strong antiferromagnetic coupling regime.

Entry	Quantity	$R_{Na-Na} = 3.5$ Å	$R_{Na-Na} = 4.0$ Å	$R_{Na-Na} = 5.0$ Å	$R_{Na-Na} = 6.0$ Å
1	E_s^{RHF}	– 323.689657	– 323.683167	– 323.665965	– 323.650500
2	E_b^{UHF}	– 323.695047	– 323.694582	– 323.692806	– 323.692111
3	E_t^{ROHF}	– 323.683151	– 323.687727	– 323.690873	– 323.691601
4	$E_t^{CCSD(T)}$	– 323.686358	– 323.690344	– 323.692373	– 323.692380
5	$E_s^{CCSD(T)}$	– 323.714863	– 323.709183	– 323.698502	– 323.693758
6	$E_s^{CCSD(T)} - E_t^{CCSD(T)}$	– 0.028505	– 0.018839	– 0.006129	– 0.001378
7	$E_s^{RHF} - E_t^{ROHF}$	– 0.006506	0.004560	+ 0.024908	+ 0.041101
8	Equation (11)	– 0.016906 (59.3 %)	– 0.011065 (58.7 %)	– 0.003616 (59.0 %)	– 0.001003 (72.8 %)
9	Equation (12)	– 0.023792 (83.5 %)	– 0.013710 (72.8 %)	– 0.003866 (63.1)	– 0.001020 (74 %)
10	Equation (13)	– 0.011896 (41.7 %)	– 0.006855 (36.4 %)	– 0.001933 (31.5 %)	– 0.000510 (37.0 %)
11	$\langle \Psi_b^{UHF} \mid S^2 \mid \Psi_b^{UHF} \rangle$	0.5927	0.7610	0.9310	0.9827

0947-6539/01/0702-0408 $ 17.50+.50/0 *Chem. Eur. J.* **2001**, *7*, No. 2

Table 2. The singlet–triplet gaps computed by means of Equations (11)–(13) for Na_2 molecules with various bond lengths. Quantities used in Equations (11)–(13) were obtained from B3LYP computations. The different bond lengths simulate antiferromagnetic couplings of various strengths. In the case of the weakest antiferromagnetic coupling, Equations (11) and (12) produce singlet–triplet gaps which are too large by a factor of ≈2. In the case of a strong antiferromagnetic coupling, Equations (11) and (13) lead to quite accurate gaps. Over the whole range of coupling strengths, the strong coupling Equation (13) yields gaps with reasonable accuracy. This arises from a cancellation of errors.[34]

Entry	Quantity	$R_{Na-Na} = 4.5$ Å	$R_{Na-Na} = 5.0$ Å	$R_{Na-Na} = 5.5$ Å	$R_{Na-Na} = 6.0$ Å
1	E_s^{B3LYP}	−324.582291	−324.575223	−324.569338	−324.564658
2	E_b^{UB3LYP}	−324.583098	−324.578676	−324.576150	−324.574791
3	$E_t^{ROB3LYP}$	−324.572403	−324.572849	−324.573023	−324.573112
4	E_t^{UB3LYP}	−324.572413	−324.572860	−324.573034	−324.573123
5	$E_s^{CCSD(T)} - E_t^{CCSD(T)}$	−0.011283	−0.006129	−0.003040	−0.001378
6	Equation (11)	−0.013384 (119%)	−0.009001 (147%)	−0.005502 (181%)	−0.003164 (230%)
7	Equation (12)	−0.021390 (190%)	−0.011654 (190%)	−0.006254 (206%)	−0.003358 (244%)
8	Equation (13)	−0.010695 (95%)	−0.005827 (95%)	−0.003127 (103%)	−0.001679 (122%)
9	$\langle \Psi_b^{UB3LYP} \mid S^2 \mid \Psi_b^{UB3LYP} \rangle$	0.4018	0.7065	0.8633	0.9387

energies E_b^{UB3LYP} (Entry 2) are lower than the energies E_s^{B3LYP} (Entry 1). Thus the symmetry-broken solution describes a system that exhibits a weak antiferromagnetic coupling. The energies $E_t^{ROB3LYP}$ and E_t^{UB3LYP} for the first excited triplet state are given in Entries 3 and 4. They were computed by means of the restricted and unrestricted open-shell formalism, respectively. We realize that the $E_t^{ROB3LYP}$ and the E_t^{UB3LYP} values are almost identical. This finding supports the notion that the use of the restricted or the unrestricted $\tilde{E}_t$ entering Equations (11)–(13) might not be decisive to obtain reasonable singlet–triplet gaps. The singlet–triplet gaps computed with the coupled-cluster method are given in Entry 5. Again, they serve as reference energies for an assessment of the accuracy of Equations (11)–(13). At the limit of a weak coupling, the general Equation (11) as well as the specified Equation (12) should hold. The data given in Entries 6 and 7, however, confirm the known result[21, 32] that Equations (11) and (12) produce singlet–triplet gaps which are too large by approximately a factor of two (230% and 244%). One reason for the insufficient accuracy of the spin-corrected Equation (11) might be that a Slater determinant Ψ_b^{UHF} composed of Kohn–Sham orbitals is used to compute $\langle \Psi_b^{UHF} \mid S^2 \mid \Psi_b^{UHF} \rangle$. Such a method has been questioned by Gräfenstein et al.,[29] and they suggest an alternative method to compute the spin contamination in unrestricted DFT computations.[29]. At the smaller distance of 4.5 Å, a stronger antiferromagnetic coupling operates and Equation (13) should hold as well as the general Equation (11). Indeed, Equations (11) and (13) produce singlet–triplet gaps with good accuracy (119% and 95%). Moreover, we observe that the strong coupling Equation (13) produces reasonable singlet–triplet gaps for the whole range of coupling strengths. Ruiz et al. used this strong coupling equation to obtain exchange coupling constants which are in good agreement with experimental values.[33] However, this agreement seems to arise from a cancellation of errors, as pointed out by Caballol et al.[34]

Theoretical results for the iminosemiquinone copper(II) complex

Applied computational method: We are primarily interested in a qualitative understanding of the interesting reactivity of complex **1**. For this purpose, we considered model compound **1′** in which the *tert*-butyl and ethyl groups are replaced by hydrogens. All computations of **1′** were performed by means of the Gaussian 98 suite of ab initio programs[23] implemented on an Origin 2000[35] We performed B3LYP[27] DFT calculations in which Becke's hybrid exchange functional (B3) and the correlation functional of Lee, Yang, and Parr (LYP) are combined. Moreover, BP86 computations were performed by the use of Becke's density gradient-corrected exchange potential (B)[36] and Perdew's correlation functional (P86).[37] All calculations were performed with a pseudopotential for the copper atom combined with the corresponding basis sets, as suggested by Preuss and co-workers.[38] The pseudopotential and the basis sets were referenced by the Gaussian keyword SDD. With a reasonable starting geometry for **1′**, we performed restricted BP86 and B3LYP computations for the singlet ground state. Subsequently, the restricted solutions were tested with respect to instabilities by means of the procedure developed by Bauernschmitt and Ahlrichs.[28] This method has been referenced in Gaussion 98 by the use of the modified keyword STABLE = OPT. The restricted solutions were found to be unstable at the starting geometry and unrestricted solutions, with a *lower* energy than the restricted ones, were found by the program. This indicates that in **1′** a weak antiferromagnetic coupling operates and the symmetry-broken formalism[5–7] can be applied. We used the symmetry-broken DFT solutions as a starting guess to find the optimized geometries for the symmetry-broken electronic state of **1′**. Subsequently, vibrational frequency calculations were performed to check for the presence of minima on the potential energy surfaces.

With the B3LYP-optimized geometry of **1′**, the energy for the unrestricted symmetry-broken solution was −921.180598 a.u. and the restricted solution had an energy of −921.142642 a.u. (Table 3). The lower energy of the symmetry-broken solution shows that a weak antiferromagnetic spin-coupling operates in **1′**. The corresponding expectation value over the total spin operator S^2 is 1.0163. Therefore, the symmetry-broken solution at the optimized B3LYP geometry seems to be an almost equal mixture of a singlet and a triplet state. The singlet–triplet gap Equations (11)–(13) were derived in the wavefunction framework; however, we applied them to **1′** in the density functional framework. We used for E_b^{UHF} the unrestricted B3LYP energy of the

Table 3. The singlet–triplet gap computed for model complex **1′**. Equation (13) almost reproduces the experimental value of 274 cm^{-1}. The general spin-corrected Equation (11) seems to be less accurate in the density functional framework. The singlet–triplet gap obtained from the restricted spin-pure DFT calculations is much too large. Moreover, an unobserved triplet ground state is predicted.

Method	E [a.u.]	$E_s - E_t$ [cm^{-1}]
E_b^{UB3LYP}	– 921.180598	
		– 224 [Eq. (13)]; – 457 [Eq. (11)]
$E_t^{ROB3LYP}$	– 921.179573	
		8105
E_s^{RB3LYP}	– 921.142642	

Table 4. Selected theoretical (BP86) bond angles of model complex **1′** and experimental bond angles of **1**.[1]

Angle	BP86 [°]	Experiment [°]
N(2)-Cu(1)-O(24)	85.9	83.8
O(13)-Cu(1)-O(24)	160.7	159.7
O(24)-Cu(1)-N(25)	95.8	96.1
N(2)-Cu(1)-O(13)	85.9	83.3
N(2)-Cu(1)-N(25)	164.1	168.3
O(13)-Cu(1)-N(25)	96.9	99.7

symmetry-broken electronic state of **1′**. For $\tilde{E}_t$ we applied the restricted open-shell B3LYP energy of the first excited triplet state of **1′**.

The crystal structure analysis indicates that **1** is nonplanar.[1] The nonplanarity is reproduced by the BP86 DFT procedure, whereas the B3LYP DFT method indicates a planar geometry. Both schemes, however, yield similar bond lengths. The B3LYP scheme produces a reasonable singlet–triplet energy gap (see the section on the "overall magnetic properties") which is too large when the BP86 procedure is employed. Therefore, we used B3LYP to obtain the singlet–triplet energy splittings, but BP86 to compute the geometry of **1′**. The good performance of the BP86 procedure to compute geometries of transition metal compounds has already been recognized by Jonas and Thiel:[39] they computed geometries and vibrational frequencies for transition metal carbonyls that are in excellent agreement with experiment.[39]

The computed geometry: The BP86-optimized bond lengths and angles of model complex **1′** are given in Figure 1 and Table 4. The computed bond lengths of **1′** are in qualitative agreement with the experimental bond lengths of **1**.[1] In particular, the bond length alternation found experimentally in the phenyl rings of **1** is reasonably reproduced by the computation. The ring carbon–carbon bonds in **1′** can be partitioned into two sets located on the left-hand side or the right-hand side of an assumed mirror plane that is perpendicular to the molecular plane. Any bond in one set corresponds to a bond in the other set, and both corresponding bond lengths are computed to be almost equal. In the crystal structure of **1**, however, the experimental bond lengths of the corresponding bonds seem to be different (Figure 1). This might be induced by the presence of the *tert*-butyl and the ethyl substituents in **1** and/or crystal packing effects. The copper atom in complex **1′** was found to be slightly out of the plane spanned by the nitrogen atoms N(2) and N(25) and the oxygen atoms O(13) and O(24).[1] The position of the Cu atom is compatible with a small distortion from the square-planar geometry towards a tetrahedral geometry. This is reflected by the computed bond angles N(2)-Cu(1)-N(25) and O(24)-Cu(1)-O(13), which are close to the experimental angles (Table 4).[1] The two phenyl rings were computed to be almost coplanar. In the crystal, however, there is angle of 26.5° between the two planes of the phenyl rings.[40]

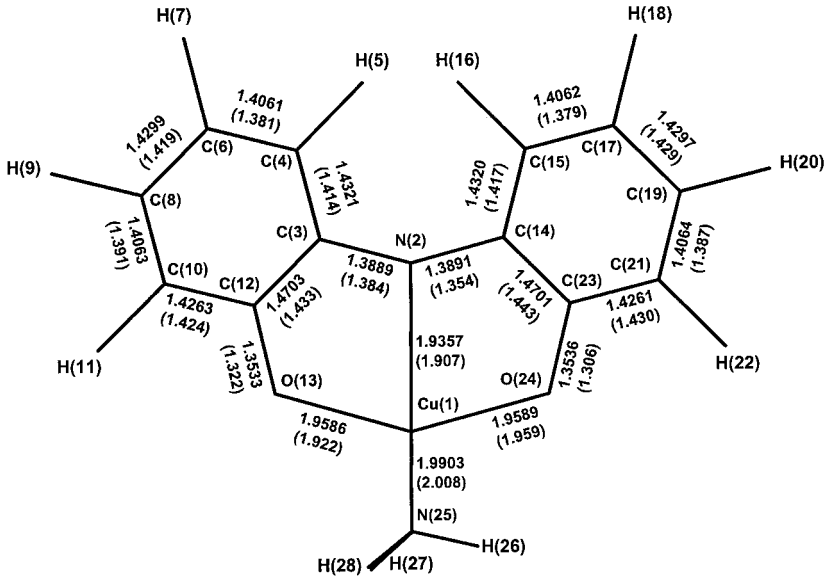

Figure 1. A comparison between the BP86-computed bond lengths for model complex **1′** and the experimental bond lengths for **1**[1] given in parentheses. The calculated bond lengths are in agreement with the experimental bond lengths. In particular, the pronounced alternation in the bond lengths within the rings is reproduced. The computation leads, however, to equal bond lengths for the bonds which are interrelated by a mirror plane assumed to be perpendicular to the molecular plane. This seems to be at variance with experiment. The nonplanarity of the Cu moiety of **1**, however, is reasonably reproduced.

The overall magnetic properties: A major objective in this work is to determine the spin multiplicity of the electronic ground state of **1′**. Relevant energy quantities are given in Table 3. They are computed at the optimized geometry calculated for the symmetry-broken electronic state. The optimized geometry of **1′** and the energy quantities have been derived in the B3LYP framework. The unrestricted energy E_b^{UB3LYP} for the symmetry-broken electronic state is the lowest energy. The energy $E_t^{ROB3LYP}$, computed within the restricted open-shell approach, locates the triplet state slightly above the symmetry-broken electronic state. When the restricted formalism is applied, a significantly higher energy, E_s^{RB3LYP}, is obtained for

0947-6539/01/0702-0410 $ 17.50+.50/0 *Chem. Eur. J.* **2001**, *7*, No. 2

the singlet ground state. The symmetry-broken formalism predicts that **1′** should have a singlet ground state (Table 3), which is in agreement with experiment.[1] We used Equation (13) to obtain a singlet–triplet gap of 224 cm^{-1} for **1′**. This value is close to the experimental value of 274 cm^{-1} derived by fitting the temperature-dependent magnetic moments of **1** to the theoretical curve based on the Heisenberg Hamiltonian.[1] By the use of the computed S^2 expectation value of 1.0163, we derived from the spin-corrected Equation (11) a singlet–triplet gap of 457 cm^{-1}. Thus, in spite of the fact that Equation (11) accounts for spin contamination, it seems to be less accurate than Equation (13). This finding agrees with our above results for the Na_2 molecules with elongated bonds. The UHF results in Table 1 illustrate that Equation (11) is more accurate than Equation (13). However, within the B3LYP framework, Equation (13) produces more accurate singlet–triplet gaps than Equation (11). This difference in the behavior of the UHF and B3LYP schemes is also in agreement with the work of Ruiz et al.[31] A spin-corrected formula that is similar to Equation (11), yields rather accurate exchange coupling constants for the model system H-He-H in the UHF framework. In the B3LYP scheme, however, a strong coupling formula similar to Equation (13) yields more accurate coupling constants.[31] The good performance of Equation (13) may arise from a cancellation of errors, as pointed out by Caballol et al.[34] The energy difference $E_s^{RB3LYP} - E_t^{ROB3LYP}$, computed in the restricted density functional formalism, produces a gap of 8105 cm^{-1} which is too large. Moreover, the electronic ground state of **1** should be a triplet state which is at variance with experiment.[1] By employing the minimized nonplanar BP86 geometry and the corresponding energy quantities, the correct singlet spin multiplicity for the electronic ground state is predicted. However, Equation (13) yields a gap of 2420 cm^{-1}, which is also too large. An even larger gap of 2968 cm^{-1} is obtained when Equation (11) is employed. Nevertheless, our results are further evidence that molecules that exhibit a weak antiferromagnetic coupling can be reasonably treated by means of the symmetry-broken formalism applied in the B3LYP framework.

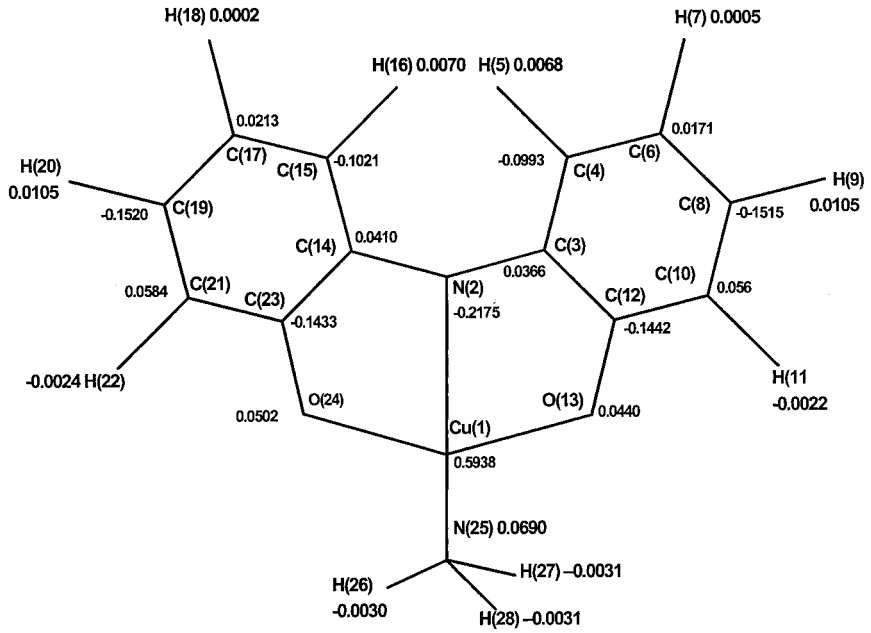

Figure 2. The Mulliken spin-density distribution for the symmetry-broken electronic state of **1′** that exhibits an overall spin density of zero. However, large local spin densities of opposite sign appear at the copper atom and the iminosemiquinone nitrogen. The antiferromagnetic coupling between these two atoms seems to dominate the antiferromagnetic coupling in **1′**.

The spin-density distribution that results from the symmetry-broken solution: In the following we consider the atomic spin densities for the symmetry-broken electronic state, although we know that they are without a physical meaning.[41] Nevertheless, it is of interest to illustrate how details of this spin-density distribution can serve to obtain qualitative information on the character of the magnetic orbitals. In Figure 2 we present the Mulliken spin populations[23] for the atoms of **1′**, as derived from the symmetry-broken B3LYP solution computed with the UB3LYP-optimized geometry. The symmetry-broken solution implies that positive and negative spin densities appear but they add up to zero. We can identify α- and β-spin densities by positive and negative spin-density values, respectively. Thus, Figure 2 shows that a large amount of α electrons is localized at the copper atom. In contrast, a large β-spin density is situated at the nitrogen atom N(2). These findings suggest that an antiferromagnetic coupling between the copper atom and the iminosemiquinone ligand is mediated by the imino nitrogen atom N(2) (Figure 2). It is instructive to consider the gross orbital spin-density population[23] at the copper atom and the next nearest atoms involved in coordination.[42] The spin density in the copper $d_{x^2-y^2}$ atomic orbital (AO) is 0.6543, which is close to the value given in Figure 2. In our computations, the xy plane is the molecular plane. Therefore, we conclude that the α electrons at the copper atom are σ electrons. A negative spin density of -0.2392 is situated in the p_z AO of the N(2) atom and a positive spin density of 0.0875 is located in the p_y AO. Therefore, the β and α electrons at the N(2) atom are π and σ electrons, respectively. At the oxygen atoms O(13) and O(24), small and almost equal amounts of α and β electrons are present which are of σ and π type, respectively. A small amount of σ electrons with α spin is located at the nitrogen atom N(25). Thus, the gross orbital spin-density populations lead to two conclusions: Firstly, the α electrons are σ electrons and they are mainly localized at the copper atom as well as at the contact atoms N(2), O(13), O(24), and N(25). Secondly, the β electrons are π electrons and they are delocalized over the atoms N(2), O(13), and O(24) of the iminosemiquinone ligand. In the following we illustrate that

these conclusions are also supported by the form of the magnetic orbitals.

The magnetic orbitals: In the section above on "overall magnetic properties", we outlined that the symmetry-broken formalism applied in the B3LYP density functional framework indicates the correct singlet spin multiplicity for the ground state of **1**. Moreover, the computed singlet–triplet energy gap is in reasonable agreement with the experimental value. In this section we suggest and apply a simple method for the determination of those MOs which are occupied by electrons involved in a weak antiferromagnetic spin coupling.

Consider two electrons with opposite spins: a strong antiferromagnetic coupling is exhibited, provided the two electrons closely approach each other. This can occur in cases in which the two electrons have the option to occupy the same spatial regions of a molecule. They occupy the same regions of space when the two electrons are located in *one* MO. In other words, a strong antiferromagnetic coupling operates when the forms of the α- and β-spin orbitals are identical. This situation is imposed in the closed-shell restricted MO procedures in which two electrons of opposite spin occupy the same MO. This restriction is appropriate for the majority of organic compounds that exhibit a strong antiferromagnetic coupling between two electrons which form a bond. However, in order to treat a weak antiferromagnetic coupling, the adopted wavefunction should permit the α and β electrons to become located in α and β MOs whose forms can be *different*. These MOs can be localized in different parts of the molecule. This local character of the MOs is the basis of the valence-bond configuration-interaction model to describe the electronic properties of transition metal dimers.[43] The symmetry-broken UHF wavefunction has the flexibility to describe a weak antiferromagnetic coupling of electron spins. However, not all electrons in the UHF wavefunction are weakly coupled. A strong antiferromagnetic coupling should exist between those α and β electrons that are located in MOs of similar shape. Thus, the forms of the α and β MOs of the UHF wavefunction should be an indicator for differentiating between strongly and weakly spin-coupled electrons. In the following, we consider the symmetry-broken electronic state of **1′** at the B3LYP-optimized geometry. The DFT computation produces 66 α and 66 β Kohn–Sham MOs which are singly occupied. Our aim is to single out the magnetic orbitals from the two MO sets. The weak antiferromagnetic coupling of the electrons in the magnetic MOs implies that they should be found in the high-energy range of α and β MOs. Therefore, we examined only the α and β MOs with numbers from 35 up to 66. We plotted the orbitals of this range[44] and we inspected their forms. For nearly any α MO one finds a matching β MO whose form is very similar. Moreover, the two matching MOs are close in energy. Therefore, we can assume that such a pair of similar MOs is occupied by two electrons that exhibit a strong antiferromagnetic coupling. Only α-MO 64 and β-MO 66 *do not match*, and their forms are given in Figure 3. We see α-MO 64 is located in the molecular plane of **1′**. It has significant d character at the copper atom; however, it is mainly localized at the nitrogen and the oxygen atoms of the iminosemiquinone ligand. It can be characterized as a Cu $d_{x^2-y^2}$ orbital with a significant contribution of the σ orbitals of the contact atoms. The β-MO 66, however, is a π MO localized preferentially at the iminosemiquinone ligand. Thus, the MOs depicted in Figure 3 are different in form, and a weak antiferromagnetic coupling exists between the electrons localized in these MOs. If this reasoning is accepted, the MOs of Figure 3 are the magnetic orbitals[45] of model complex **1′**. They characterize **1′** as a singlet diradical and only a small energy is required to invert the spins that lead to the triplet state.

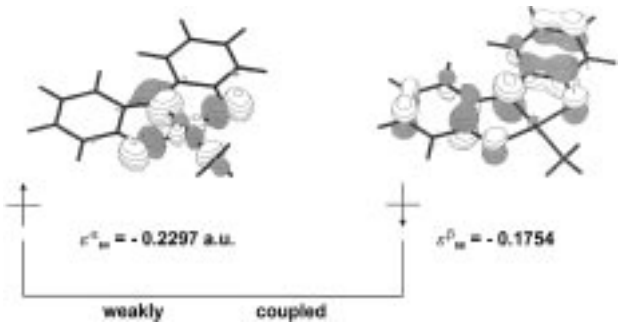

Figure 3. The two magnetic orbitals of the model compound **1′**. Both orbitals are singly occupied with electrons of opposite spin. The orbitals are preferentially localized at the iminosemiquinone ligand and they are of σ and π type. Because of their different spatial orientation, the antiferromagnetic coupling between the two electrons is only weak. ε is the energy of the singly occupied molecular orbital.

Form of the magnetic orbitals and reactivity: In the previous section we identified the B3LYP magnetic orbitals of model complex **1′**. In this section we use the form of the magnetic orbitals to obtain some qualitative information on the reactivity of **1′**. Figure 3 shows the magnetic α orbital (MO 64) is preferentially localized at the imino nitrogen and the two carbonyl oxygens of the iminosemiquinone ligand. The copper d orbital and the sp orbital of the attached NH_3 group contribute to a lesser extent. The magnetic β orbital (MO 66) is a π orbital preferentially localized at the iminosemiquinone ligand. In the following, we are interested in those spatial regions of **1′** in which the weakly coupled α and β electrons prefer to be *simultaneously* localized. For this purpose, we consider the two-electron density function $\rho^{\alpha\beta}(1,2)$ that arises from a Slater determinant $\Psi(1,2)$ composed of the two magnetic MOs ϕ^α and ϕ^β. By the use of such a simple one-determinantal wavefunction, $\rho^{\alpha\beta}(1,2)$ is entirely determined by the two one-electron density functions ρ^α and ρ^β.[46] Therefore, we can write Equation (14):

$$\rho^{\alpha\beta}(1,2) = \int\Psi(1,2)\Psi(1,2)\mathrm{d}\sigma(1)\mathrm{d}\sigma(2) = \rho^\alpha(1)\rho^\beta(2) = \phi^\alpha(1)^2\phi^\beta(2)^2 = [\phi^\alpha(1)\phi^\beta(2)]^2 \quad (14)$$

The integration is performed over the two spin variables $\sigma(1)$ and $\sigma(2)$.[46] We see, $\rho^{\alpha\beta}(1,2)$ should have large functional values in those spatial regions in which the two-electron product function $\phi^\alpha(1)\phi^\beta(2)$ is large. These are the regions in which ϕ^α and ϕ^β have large functional values. In Figure 4 we have schematically represented the spatial regions where ϕ^α and ϕ^β are large. Thus, the spatial regions in which to *simultaneously* find the two weakly spin-coupled electrons are

0947-6539/01/0702-0412 $ 17.50+.50/0 *Chem. Eur. J.* **2001**, *7*, No. 2

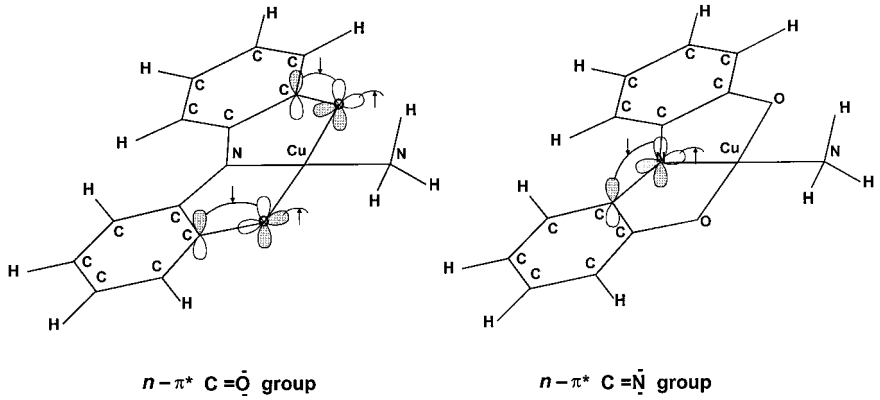

Figure 4. Spatial regions in the iminosemiquinone ligand in which the two weakly coupled electrons prefer to be located *simultaneously*. These regions are determined by the form of the magnetic orbitals. The electronic structures around the oxygen and nitrogen atoms resemble the electronic structures of the $n-\pi^*$ states of the carbonyl and the imino groups, respectively.

near the carbonyl and the N–C groups of the iminosemiquinone ligand. This small distance between the weakly spin-coupled electrons implies that the two-electron exchange integral over the magnetic orbitals[6c] should be large. Therefore, one should expect that the ferromagnetic contribution[6c] to the exchange coupling constant is large. As indicated by Figure 4, the β and α electrons are localized out and in the molecular plane, respectively. Furthermore, we realize that the two MO occupations resemble the MO occupation pattern used to qualitatively describe the singlet excited $n-\pi^*$ states of the carbonyl ($R_2C{=}O$) and of the imino ($R_2C{=}NH$) groups.[47] Thus, for the singlet ground state of model complex **1′**, which exhibits a weak antiferromagnetic coupling, the $n-\pi^*$ state photochemistries of the $R_2C{=}O$ and of the $R_2C{=}NH$ groups should be relevant. One of the efficient photoreactions of the $n-\pi^*$ excited $R_2C{=}O$ group is hydrogen-atom abstraction from molecules which are hydrogen-atom donors.[48] Hydrogen-atom abstraction occurs from the triplet[49] and singlet[50] excited $n-\pi^*$ states. Photochemical hydrogen-atom abstractions for the isoelectronic $R_2{=}NH$ group were also observed.[51] The $n-\pi^*$ state of the $R_2{=}NH$ group, however, seems not to be the reactive electronic state and reactions are less efficient.[52] The electron in the magnetic π orbital of **1′** is higher in energy than the electron in the magnetic σ orbital (Figure 3). The high energy of the π electron implies that **1′** should be rather reactive. One possible reaction pathway is to abstract a nearby hydrogen atom with an electron of opposite spin. In this way the weakly coupled π electron succeeds in becoming paired in a newly formed σ bond. Thus, the form and the energy of the magnetic π orbital (Figure 3) suggests that hydrogen-atom migration towards the iminosemiquinone ligand is an important reaction pathway for complex **1**. Probably, hydrogen-atom migration towards the carbonyl oxygen of the iminosemiquinone ligand prevails. Hydrogen-atom abstraction is the reaction proposed to be rate determining in the aerobic oxidation of alcohols catalyzed by complex **1** (Scheme 1).[1] This proposal has been experimentally substantiated by a pronounced kinetic isotope effect on the overall rate constants k for the oxidation process. If the α hydrogens of the benzyl alcohol are selectively replaced by deuterium, a k_H/k_D ratio of eight was determined.[1] This shows that the α hydrogens of the benzyl alcohol are involved in the rate-determining hydrogen-atom abstraction.[1] We find that this notion is also supported by the form of the magnetic orbitals.

Properties of the triplet state: In the previous section we obtained results for model complex **1′** that are based on the electronic properties of the B3LYP symmetry-broken electronic state. A simple scheme was applied to determine magnetic orbitals occupied by electrons that exhibit a weak antiferromagnetic coupling. The form of these orbitals supports the qualitative conclusion that the carbonyl groups of the ligand are prone to performing hydrogen-atom abstraction. The experiment indicates that the electronic ground state of **1** is a singlet state.[1] The exchange coupling constant of $J = -137\ cm^{-1}$, however, indicates that during a chemical reaction, the lowest triplet state of **1** is easily accessible. Thus, for a qualitative understanding of the reactivity of **1** it is mandatory to analyze the lowest triplet state as well. Table 1 shows that for the model Na_2 molecules the restricted open-shell energies for the lowest triplet state E_t^{ROHF} are very close to the coupled-cluster energies $E_t^{CCSD(T)}$. Therefore, we can hope that the lowest triplet state of complex **1′** is also well described by the restricted open-shell DFT approach. We used the ROB3LYP/SDD level[23] of theory to optimize the geometry of the lowest triplet state of **1′**. The calculated bond lengths for the triplet state are very similar to the bond lengths calculated for the symmetry-broken electronic state. This finding shows that unpairing the weakly coupled electrons in the singlet state has only a marginal effect on the electron distribution that determines the geometry. The overall spin density, however, is strongly affected. This is reflected by the atomic Mulliken spin-density distribution[23] for the triplet state as (Figure 5). The largest spin density is computed for the copper atom. Appreciable values are also found at the nitrogen and the two carbonyl oxygens of the iminosemiquinone ligand. In the restricted open-shell formalism the spin densities for the triplet state are determined by the two singly occupied MOs that carry electrons of parallel spin. These MOs are the α orbitals 66 and 67 depicted in Figure 6. We realize that their forms are virtually identical to the forms of the magnetic orbitals for the symmetry-broken electronic state (Figure 3). Even their relative energetic ordering is similar. These findings illustrate that on moving from the symmetry-broken electronic state to the first excited triplet state only one spin is inverted. The space parts of the magnetic orbitals, however, should remain the same for the symmetry-broken formalism and for the first excited triplet state. The similarity of the orbitals shown in Figures 3 and 6 confirms that we identified the correct magnetic orbitals. Moreover, from Figure 6 one can conclude that the spatial regions for *simultaneously*

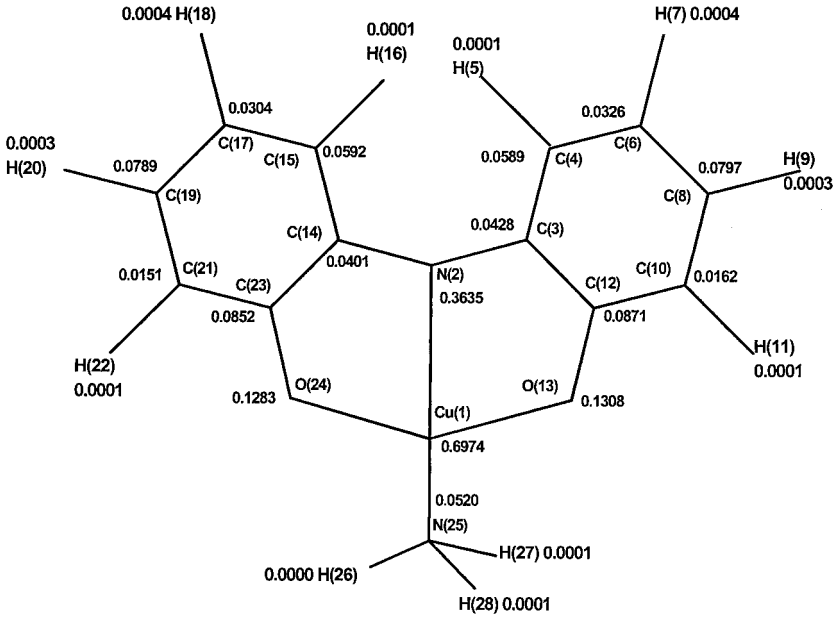

Figure 5. The Mulliken spin-density distribution for the lowest triplet state of the model complex **1′**. Large spin densities are computed for the copper atom and the nitrogen of the iminosemiquinone ligand.

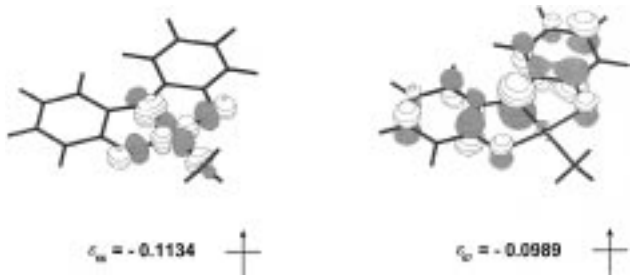

Figure 6. The two singly occupied orbitals for the lowest triplet state of model complex **1′**. Their form is almost identical to the form of the magnetic orbitals for the symmetry-broken electronic state (Figure 3). This similarity supports the notion that the exchange coupling in **1′** can be qualitatively rationalized by means of the two magnetic orbitals depicted in Figure 3. ε is the energy of the singly occupied molecular orbital.

finding two electrons with α spins are identical to the regions in which two electrons with opposite spin can be found (Figure 4). These regions are situated in a fashion that simulates a triplet $n-\pi^*$ excitation. Such excitations of the carbonyl groups are known to induce hydrogen-atom abstractions.[48] Because of the longer lifetimes of the triplet states they are more efficient for hydrogen-atom abstractions than singlet states.[50] In complex **1** both electronic states are easily accessible, as indicated by the small singlet–triplet gap of 274 cm^{-1}. In the organic photochemistry both electronic states are found to induce hydrogen-atom abstraction. Therefore, this reaction pathway should be important. Our qualitative theoretical analysis supports the proposal[1] that hydrogen-atom abstraction is the rate-determining step in the catalytic oxidation of alcohols (Scheme 1).

Conclusions

We have applied the symmetry-broken formalism[5] to elucidate the electronic structure of the iminosemiquinone copper(II) catalyst **1**. A characteristic feature of our analysis is that we applied analytic formulas derived within the unrestricted Hartree–Fock scheme, but applied energies computed within the unrestricted DFT framework.[7] Moreover, the unrestricted Kohn–Sham orbitals were used as a substitute for the UHF MOs. As in previous work,[7] this methodology also leads to the correct singlet spin multiplicity of **1′**. Moreover, the observed singlet–triplet energy gap was reasonably reproduced, provided the B3LYP density functional scheme is applied. We were particularly interested in the determination of the two magnetic orbitals which are singly occupied by two electrons that exhibit a weak antiferromagnetic coupling. We determined the magnetic orbitals by pursuing the notion that the shape of these orbitals should be different. This difference in shape prevents the close approach of the two spin-coupled electrons to one another to result in a weak antiferromagnetic coupling. The shape argument leads to a simple method to distinguish between MOs carrying strongly or weakly spin-coupled electrons. On inspection of the forms of the occupied unrestricted Kohn–Sham orbitals, we find that almost any α orbital matches a β orbital in form and energy. Those orbital pairs contain electrons, which exhibit a strong antiferromagnetic coupling. The only exception are the two magnetic orbitals represented in Figure 3. The $\alpha(\beta)$ orbital does not find a matching partner in the set of the occupied $\beta(\alpha)$ orbitals and this implies a weak antiferromagnetic coupling between the spins of the electrons in the magnetic orbitals. Consequently, atoms in a molecule that carry those unpaired spins are prone to reactions which lead to a more effective spin pairing. Guided by the form of the magnetic orbitals, we determined qualitatively that such a reaction of **1′** can be a hydrogen-atom abstraction. This finding corroborates the suggestion of Wieghardt and co-workers that a hydrogen-atom abstraction reaction for **1** should be the rate-determining step in the catalytic cycle given in Scheme 1.[1] Our theoretical results support the notion that the form of the magnetic orbitals might be a qualitative tool for the prediction of the reactivity of compounds that exhibit a weak antiferromagnetic coupling.

Acknowledgements

The interesting and stimulating discussions with Prof. V. Staemmler are gratefully appreciated. We thank one referee for his constructive comments and several helpful suggestions.

[1] P. Chaudhuri, M. Hess, T. Weyermüller, K. Wieghardt, *Angew. Chem.* **1999**, *111*, 1165; *Angew. Chem. Int. Ed.* **1999**, *38*, 1095.

[2] In the case of Fe_3 clusters, this is mentioned in: L. Noodleman, D. A. Case, *Adv. Inorg. Chem*. **1994**, 38, 423 (particularly p. 454) and references cited therein; for model Fe_2-S clusters, the form of the magnetic orbitals are given in: L. Noodleman, E. J. Baerends, *J. Am. Chem. Soc*. **1984**, *106*, 2316, in particular, Figure 2,; See also: ref. [5b] and A. Bencini, S. Midollini, *Coord. Chem. Rev*. **1992**, *120*, 87 (particularly p. 127).

[3] C. Wang, K. Fink, V. Staemmler, *Chem. Phys.* **1994**, *201*, 87; K. Fink, R. Fink, V. Staemmler, *Inorg. Chem*. **1994**, *33*, 6219; C. Kolczewski, K. Fink, V. Staemmler, *Int. J. Quant. Chem.* **2000**, *76*, 137.

[4] K. Fink, C. Wang, V. Staemmler, *Inorg. Chem*. **1999**, *38*, 3847.

[5] a) L. Noodleman, *J. Chem. Phys.* **1981**, *74*, 5737; b) L. Noodleman, E. R. Davidson, *Chem. Phys.* **1986**, *109*, 131.

[6] a) K. Yamaguchi, T. Tsunekawa, Y. Toyota, T. Fueno, *Chem. Phys. Lett*. **1988**, *143*, 371; b) J. R. Hart, A. K. Rappe, S. M. Gorun, T. H. Upton, *Inorg. Chem*. **1992**, *31*, 5254; c) J. R. Hart, A. K. Rappe, S. M. Gorun, T. H. Upton, *J. Phys. Chem*. **1992**, *96*, 6264.

[7] For recent work see, for example: a) T. C. Brunhold, E. I. Solomon, *J. Am. Chem*. Soc. **1999**, *121*, 8277; J. Cano, E. Ruiz, P. Alemany, F. Lloret, S. Alvarez, *J. Chem. Soc. Dalton Trans.* **1999**, 1669; I. Demachy, Y. Jean, A. Lledo's, *Chem. Phys. Lett*. **1999**, *303*, 621; A. Caneschi, F. Fabrizi de Biani, L. Kloo, P. Zanello, *Int. J. Quant. Chem*. **1999**, *72*, 61; J. H. Rodrigues, D. E. Wheeler, J. K. McCusker, *J. Am. Chem*. **1998**, *120*, 12051; A. Lledo's, Y. Jean, *Chem. Phys. Lett*. **1998**, *287*, 243; J. Cano, P. Alemany, S. Alvarez, M Verdaguer, E. Ruiz, *Chem. Eur. J.* **1998**, *4*, 476; H. Kuramochi, L. Noodleman, D. A. Case, *J. Am. Chem. Soc*. **1997**, *119*, 11442; b) A. Bencini, F. Totti, C. A. Daul, P. Doclo, P. Fantucci, V. Barone, *Inorg. Chem*. **1997**, *36*, 5022.

[8] For a thorough discussion of the properties of the UHF wavefunction, see, for example: A. Szabo, N. S. Ostlund, *Modern Quantum Chemistry*, McGraw-Hill, New York, **1982**, Section 3.8, in particular p. 207.

[9] See for example: a) ref. [5a] in particular p. 5738; b) L. Noodleman, C. Y. Peng, D. A. Case, J.-M. Mouesca, *Coord. Chem. Rev*. **1995**, *144*, 199 (particularly p. 212).

[10] See for example: ref. [8], pp. 104–107.

[11] See ref. [5a], Equation (34) which is the formula for the exchange coupling constant *J*.

[12] The same is carried out in perturbation theory: the perturbed first-order wavefunction is expanded into the complete set of unperturbed eigenfunctions. See, for example: H. Eyring, J. Walter, G. E. Kimball, *Quantum Chemistry*, Wiley, New York, **1964**, p. 93, Equations (7)–(10).

[13] H and S^2 commute. Therefore, H and S^2 share the same set of eigenfunctions. See, for example: W. Kutzelnigg, *Einführung in die Theoretische Chemie*, Band 1, Verlag Chemie, Weinheim, **1975**, p. 33.

[14] a) A. T. Amos, G. G. Hall, *Proc. R. Soc. London Ser. A* **1961**, *263*, 483 (in particular p. 490); b) see also ref. [8], p. 106, Equation (2.270).

[15] See, for example: F. L. Pilar, *Elementary Quantum Chemistry*, McGraw-Hill, New York, **1968**, p. 288, Figure 11-1.

[16] L. Noodleman, D. A. Case, *Adv. Inorg. Chem*. **1994**, *38*, 423, [in particular p. 431, Eq. (19)]; see also ref. [9b] p. 214, Equation (2).

[17] A. A. Ovchinnikov, J. Labanowski, *Phys. Rev. A*, **1996**, *53*, 3946, in particular Figures 1 and 2.

[18] J. M. Wittbrodt, H. B. Schlegel, *J. Chem. Phys.* **1996**, *105*, 6574.

[19] See ref. [14a] p. 491, Table 2.

[20] See ref. [17], Equation (6).

[21] C. Adamo, V. Barone, A. Bencini, F. Totti, I. Ciofini, *Inorg. Chem*. **1999**, *38*, 1996, Equation (6).

[22] R. Caballol, O. Castell, F. Illas, I. de P. R. Moreira, J.-P. Malrieu, *J. Phys. Chem. A* **1997**, *101*, 7860, in particular the simplified Equation (11) that leads to Equation (3).

[23] M. J. Frisch, G. W. Trucks, H. B. Schlegel, G. E. Scuseria, M. A. Robb, J. R. Cheeseman, V. G. Zakrzewski, J. A. Montgomery, Jr., R. E. Stratmann, J. C. Burant, S. Dapprich, J. M. Millam, A. D. Daniels, K. N. Kudin, M. C. Strain, O. Farkas, J. Tomasi, V. Barone, M. Cossi, R. Cammi, B. Mennucci, C. Pomelli, C. Adamo, S. Clifford, J. Ochterski, G. A. Petersson, P. Y. Ayala, Q. Cui, K. Morokuma, D. K. Malick, A. D. Rabuck, K. Raghavachari, J. B. Foresman, J. Cioslowski, J. V. Ortiz, B. B. Stefanov, G. Liu, A. Liashenko, P. Piskorz, I. Komaromi, R. Gomperts, R. L. Martin, D. J. Fox, T. Keith, M. A. Al-Laham, C. Y. Peng, A. Nanayakkara, C. Gonzalez, M. Challacombe, P. M. W. Gill, B. Johnson, W. Chen, M. W. Wong, J. L. Andres, C. Gonzalez, M. Head-Gordon, E. S. Replogle, J. A. Pople, *Gaussian 98*, *Revision A.5*, Gaussian, Pittsburgh PA, **1998**.

[24] A. D. McLean, G. S. Chandler, *J. Chem. Phys.* **1980**, *72*, 5639; R. Krishnan, J. S. Binkley, R. Seeger, J. A. Pople, *J. Chem. Phys*. **1980**, *72*, 650.

[25] R. Seeger, J. A. Pople, *J. Chem. Phys.* **1977**, *66*, 3045.

[26] J. A. Pople, M. Head-Gordon, K. Raghavachari, *J. Chem. Phys.* **1987**, *87*, 5968.

[27] A. D. Becke, *J. Chem. Phys.* **1993**, *98*, 5648; C. Lee, W. Yang, R. G. Parr, *Phys. Rev. B* **1988**, *37*, 785.

[28] R. Bauernschmitt, R. Ahlrichs, *J. Chem. Phys.* **1996**, *104*, 9047.

[29] J. Gräfenstein, A. M. Hjerpe, E. Kraka, D. Cremer, *J. Phys. Chem. A* **2000**, *104*, 1748.

[30] *Tables of Interatomic Distances and Configurations in Molecules and Ions*, The Chemical Society, London, **1958**, S7.

[31] E. Ruiz, J. Cano, S. Alvarez, P. Alemany, *J. Comp. Chem*. **1999**, *20*, 1391.

[32] See for example: ref. [22] in particular Tables 2 and 3.

[33] E. Ruiz, P. Alemany, S. Alvarez, J. Cano, *J. Am. Chem. Soc*. **1997**, *119*, 1297.

[34] See ref. [22] in particular p. 7864.

[35] We thank R. Trinoga for implementing Gaussian 98 on the Origin 2000 computer.

[36] A. D. Becke, *Phys. Rev. A* **1988**, *38*, 3098.

[37] J. P. Perdew, *Phys. Rev. B* **1986** *33*, 8822.

[38] T. H. Dunning, P. J. Hay in *Modern Theoretical Chemistry*, *Vol. 3* (Ed.: H. F. Schaeffer, III), Plenum, New York, **1977**; M. Dolg, U. Wedig, H. Stoll, H. Preuss, *J. Chem. Phys.* **1987**, *86*, 866.

[39] V. Jonas, W. Thiel, *J. Chem. Phys.* **1995**, *102*, 8474.

[40] We thank Dr. T. Weyhermüller for providing this information.

[41] For a symmetry-broken state, two equivalent Kohn–Sham determinants always exist in which the α- and β-spin densities are interchanged.[22, 30] Linear combination of the two determinants leads to a solution where the spin densities vanish.

[42] We thank one referee for making this suggestion.

[43] E. I. Solomon, F. Tuczek, D. E. Root, C. A. Brown, *Chem. Rev*. **1994**, *94*, 827.

[44] The MOs were plotted by means of the public-domain program MOLDEN.

[45] See, for example: O. Kahn, *Molecular Magnetism*, VCH Publishers, **1993**, Chapter 8

[46] See, for example for the two-electron case: W. Kutzelnigg, *Einführung in die Theoretische Chemie*, *Band 1*, Verlag Chemie, Weinheim, **1975**, in particular p. 204. The *n*-electron case is mentioned for example in: R. McWeeny, *Methods of Molecular Quantum Mechanics*, Academic Press, London, **1996**, in particular p. 126, Equation (5.3.9).

[47] See, for example: A. Gilbert, J. Baggot, *Essentials of Molecular Photochemistry*, Blackwell, Oxford, **1991**, Sect. 2.5.1., pp. 42–43, p. 40, and Figure 9.10.

[48] See for example: a) N. J. Turro, *Modern Molecular Photochemistry*, Benjamin, Menlo Park, **1978**, pp. 367–372; b) ref. [47], pp. 302–328, for intramolecular hydrogen abstraction, see pp. 310–328.

[49] See, for example: J. A. Barltrop, J. D. Coyle, *Excited States in Organic Chemistry*, Wiley, London, **1975**, pp. 190–200 (in particular p. 191).

[50] This holds for the intramolecular hydrogen-atom abstractions: See for example: J. A. Barltrop, J. D. Coyle, Excited States in Organic Chemistry, Wiley, London, **1975**, pp. 193–200, in particular p. 194, Table 7.3.

[51] See A. Gilbert, J. Baggot, *Essentials of Molecular Photochemistry*, Blackwell, Oxford, **1991**, pp. 412–415.

[52] See A. Gilbert, J. Baggot, *Essentials of Molecular Photochemistry*, Blackwell, Oxford, **1991**, p. 413.

Received: February 8, 2000
Revised version: July 20, 2000 [F2287]